Photosynthetic and water transport strategies of plants along a tropical forest aridity gradient: a test of optimality theory

Corresponding author:

Huanyuan Zhang-Zheng, (0000-0003-4801-8771) (huanyuan.zhangzheng@gmail.com)

Author list:

Huanyuan Zhang-Zheng1, (0000-0003-4801-8771)

Yadvinder Malhi1, (0000-0002-3503-4783)

Agne Gvozdevaite1,

Theresa Peprah4,

Mickey Boackye3,

Kasia Ziemińska2, (0000-0001-7750-4758)

Stephen Adu-Bredu4,

Jesús Aguirre-Gutiérrez 1,(0000-0001-9190-3229)

David Sandoval 5,

Colin Prentice 5, (0000-0002-1296-6764)

Imma Oliveras1,2, (0000-0001-5345-2236)

1 Environmental Change Institute, School of Geography and the Environment, University of Oxford, Oxford, United Kingdom,

2 AMAP (Botanique et Modelisation de l'Architecture des Plantes et des Végétations), CIRAD, CNRS, INRA, IRD,Université de Montpellier, Montpellier, France

3 Department of Environmental Science, Policy, and Management, University of California, Berkeley, CA, 94720, USA

4 Forestry Research Institute of Ghana, Council for Scientific and Industrial Research, Kumasi, Ghana

5 Georgina Mace Centre for the Living Planet, Department of Life Sciences, Imperial College London, Silwood Park Campus, Buckhurst Road, Ascot, SL5 7PY, UK

Word Count

Total word count for the main body of the text: 5426

Summary: 200

Introduction: 707

Materials and Methods: 2491

Results: 1029

Discussion: 999 (18.4% of total word count)

Number of figures:2 (all in colour)

Number of table: 1 (all in colour)

Supporting information is provided in another document.

Keywords

Optimality; photosynthesis; aridity; plant functional traits; plant hydraulics; xylem hydraulics

Summary

(1) The research conducted, including the rationale

The direct effect of aridity on photosynthetic and water-transport strategies is not easy to discern in global analyses because of large-scale correlations between precipitation and temperature. We analyze tree traits collected along an aridity gradient in Ghana, West Africa, that shows little temperature variation, in an attempt to disentangle thermal and hydraulic influences on plant traits.

(2) Methods

Predictions derived from optimality theory of the variation of key plant traits along the gradient are tested with field measurements.

(3) Results

Most photosynthetic traits show trends consistent with optimality-theory predictions, including higher photosynthetic rates in the drier sites, and an association of higher photosynthetic rates with greater respiration rates and greater water transport. Leaf economic and hydraulic traits show less consistency with theory or global-scale pattern, especially predictions based on xylem efficiency-sfatety trafeoff. Nonetheless, the link between photosynthesis and water transport still holds: species (predominantly deciduous species found in drier sites) with both higher sapwood-to-leaf area ratio (AS/AL) and potential hydraulic conductivity (Kp), implying higher transpiration, tend to have both higher photosynthetic capacity, and lower leaf-internal CO_2.

(4) Conclusions

These results indicate that aridity is an independent driver of spatial patterns of photosynthetic traits, while plants show a diversity of water-transport strategies along the aridity gradient.

Plain language summary: Along an aridity gradient in Ghana, West-Africa, we used optimality theory to explain why higher photosynthetic rates should be found at drier places and how plants arrange water transportation to support quicker photosynthesis at the drier site. We also reported surprising data-theory inconsistency for some hydraulic traits along the aridity gradient where further research is needed.

Introduction

Three key photosynthetic processes are frequently considered when seeking to understand plants photosynthesis strategies: light availability and electron transport; aridity and water transport; and CO_2 concentration and carboxylation (Farquhar et al., 2001). Plants capacities in these processes vary considerably along environmental gradients (Wang *et al.*, 2017a; Bahar *et al.*, 2017; Yang *et al.*, 2019; Oliveras *et al.*, 2020). Recently, many efforts have been made to propose universal rules to explain worldwide plant photosynthetic strategies, frequently cited as 'optimality theories', which could serve as a basic theoretical framework for vegetation carbon modelling and enable quantitative predictions of key photosynthetic traits (Franklin *et al.*, 2020; Harrison *et al.*, 2021).

One of the main challenges confronting these universal theories is to explain the 'pure' effect of aridity on photosynthesis (Rogers *et al.*, 2017). Such challenges become particularly pressing in the context of climate as greater atmospheric dryness (water vapour deficit, VPD) is predicted for most places (Neelin *et al.*, 2006; Grossiord *et al.*, 2020a; Bauman *et al.*, 2022), which may strongly influence photosynthesis and hence the carbon cycle (Canadell *et al.*, 2021). However, the theoretical expectation for the impact of aridity on plant traits based on optimality theories has not been summarized and tested. Most current earth systems models predict a negative relationship between photosynthesis (denoted by CO_2 assimilation rate per leaf area, A_{area}) and VPD simply due to the closing of stomata without incorporating the dynamics of photosynthetic capacity (denoted by electron-transport capacity, J_{max25} and Rubisco carboxylation capacity standardized to 25 degree celsius, V_{cmax25}) (Wang *et al.*, 2017a; Green *et al.*, 2020). On the contrary, a study focusing on Amazonia argued that higher VPD increases photosynthetic capacity which

94 counteracts the reduced conductivity, leading to higher photosynthesis under drier climates
95 (Restrepo-Coupe *et al.*, 2013; Green *et al.*, 2020). However, a global study found the above pattern
96 only exists in wet ecosystems and higher VPD reduces photosynthesis overall (Fu *et al.*, 2022)
97 although globally higher V_{cmax25} was indeed found for plants grown in drier sites (Peng *et al.*, 2021).
98 Under experimental conditions, CO_2 assimilation was found to be lower under high VPD (Long &
99 Woolhouse, 1978; Dai *et al.*, 1992; Cunningham, 2005).

100 With such mixed evidence in the literature, the stand-alone effect of aridity on photosynthesis still
101 remains unclear. There are two particular challenges. First, on a large spatial scale, aridity can be
102 confounded with temperature (especially when VPD is used as a metric of aridity). Temperature
103 is a stronger driver of photosynthesis than aridity (Smith *et al.*, 2019; Peng *et al.*, 2021), but few
104 studies try to disentangle aridity from temperature (Grossiord *et al.*, 2020a). Second, the effect of
105 VPD can be confounded with soil water availability. Optimality theory predicted higher Vcmax
106 and A_{area} under higher VPD (Smith *et al.*, 2019) but it is unclear how plants in drier environments
107 arrange water transportation to support higher $A_{area.}$ A comprehensive theoretical framework is
108 lacking to incorporate the effect of VPD on all leaf-level photosynthesis processes (light, water
109 and CO_2) with full consideration of water delivery to leaves (Mencuccini *et al.*, 2019a).

110 Here, we examine a dataset of detailed traits measurements along an aridity gradient in West
111 African forests to disentangle the effect of aridity on photosynthesis from temperature and to
112 explain the effect with optimality theory. The key questions we address are: (1) do drier
113 environments have higher photosynthesis rates and how do aridity and photosynthesis interact? (2)
114 If photosynthetic rates are higher in arid environments, as predicted by optimality theory, how do
115 plants arrange greater water transportation, given greater water stress in drier places? To answer
116 these questions, we adopted a theory-data comparison approach where we first review the
117 expectation of recent 'universal' theories and deduced 16 testable predictions (some of which have
118 previously been tested but with confounding results). We then examined the consistency between
119 each prediction and field measurement along the aridity gradient (Table 1). Consistency would
120 give field-observed patterns a mechanistic explanation and reinforce the stand-alone impact of
121 aridity on the corresponding trait, while inconsistency would imply weakness of the theory and
122 possible confounding interactions between aridity and other climate variables. Before closing the

123 paper, we summarize the consistency and inconsistency with an integrated theoretical framework
124 to address and explore the 'pure' effect of aridity on photosynthesis.

125 ## Description of theory and hypotheses development

126 'Optimality theory' was developed recently with the assumption that plants can optimize
127 photosynthesis and minimize maintenance costs according to their living environments by
128 optimizing investment in the above processes, which provides a universal explanation of the
129 variation of photosynthetic strategies under different growing environments (Prentice *et al.*, 2014;
130 Wang *et al.*, 2017b; Mencuccini *et al.*, 2019a; Stocker *et al.*, 2020; Xu *et al.*, 2021). Although the
131 above-cited studies have tested the theories on global scales and along elevation gradients,
132 discussion and validation of these theories along other abiotic gradients, such as aridity gradients,
133 are still lacking. Therefore, we first review the implication of such theories on plants
134 photosynthetic strategies along aridity gradients.

135 In drier sites, higher VPD increases potential transpiration per unit leaf area. As predicted by the
136 'least-cost hypothesis' (Wright *et al.*, 2001, 2003; Medlyn *et al.*, 2011; Prentice *et al.*, 2014), plants
137 can compensate for high water costs in dry climates by keeping stomata relatively closed. Thus, in
138 drier sites, plants are expected to have lower leaf internal CO_2 concentration (c_i), lower internal-
139 to-external CO_2 ratio (c_i/c_a) and lower stomatal conductance (g_s). The 'coordination hypothesis'
140 (Beerling & Quick, 1995; Maire *et al.*, 2012; Walker *et al.*, 2014) assumes equilibrium between
141 Rubisco-limited photosynthesis rates (A_C) (depending on V_{cmax25} and c_i) and electron transport-
142 limited photosynthesis rates (A_J) (depending on J_{max25} and leaf absorbed PPFD) (see the
143 quantitative expression in (Wang *et al.*, 2017b; Smith *et al.*, 2019; Stocker *et al.*, 2020)). To
144 maintain such an equilibrium, plants in drier sites are expected to have larger V_{cmax25} to compensate
145 for the lower c_i. Otherwise, A_C would be lower than A_J resulting in unused capacity for electron
146 transport (J_{max25}). To sum up, lower c_i but higher V_{cmax25} is expected toward drier sites if J_{max25}
147 stays constant (in which case A_J would be slightly lower due to smaller c_i).

148 In reality, toward drier sites, it is common to see higher leaf absorbed photosynthetic photon flux
149 density (I_{abs}) because of less cloud cover and more open canopies. Considering an additional
150 optimality criterion that J_{max25} is acclimated to I_{abs} (Smith *et al.*, 2019), supported by multiple

151 experiments (Björkman, 1981; Ögren, 1993), we would expect higher J_{max25} in drier sites, which
152 further encourages higher V_{cmax25} (see above paragraph). Higher J_{max25} and V_{cmax25} would give rise
153 to higher A_C and A_J. All the above would lead to higher leaf photosynthetic protein cost, hence
154 higher leaf dark respiration (Rd), and higher transpiration stream maintenance cost, hence higher
155 stem respiration per leaf area (Rs) (Prentice *et al.*, 2014). Note that R_s is stem respiration per leaf
156 area (R_{stem_leaf} hereafter), different from the commonly reported stem respiration per stem area
157 (R_{stem_stem}). Some of the above predictions have been seen on global scale; for example, higher R_d
158 has been found in drier sites (Wright *et al.*, 2001; Atkin *et al.*, 2015) and higher assimilation rate
159 has been reported from drier sites (Maire *et al.*, 2015).

160 It is worth noting that V_{cmax25}, g_s and c_i here are discussed as an overall value for a forest stand,
161 disregarding diurnal variation and intraspecific variation (Stangl *et al.*, 2019; Han *et al.*, 2022). At
162 the species or individual scales, there is a positive correlation between A_{sat} (light-saturated
163 assimilation rate at 400 ppm), V_{cmax25}, g_s and c_i (Wright *et al.*, 2003; Prentice *et al.*, 2014), instead
164 of the opposite trend of V_{cmax25} and c_i/c_a as discussed above regarding spatial variation only.

165 Photosynthesis strategies predicted by the optimality theory above can be linked with xylem water
166 transportation strategies via stomatal behaviour, as given by Fick's law,

167 $$g_s = A_{area} / (ca - ci) \quad (1)$$

168 Where g_s is stomatal conductance (umol CO_2 m-2 s-1), A_{area} is CO_2 assimilation rate per leaf area
169 (umol CO2 m2 s-1), and leaf internal (ci, ppm) and external (ca, ppm) CO_2 concentration

170 We focus on daytime conditions that produce maximum rates of transpiration and photosynthesis,
171 when water loss through stomata must equal water transport through xylem (Brodribb *et al.*, 2002;
172 Xu *et al.*, 2021):

173 $$E = 1.6\ gs\ VPD / Patm = Ks\ \Delta\Psi max\ AS/AL\ / h \quad (2)$$

174 Where Patm is atmospheric pressure (Mpa), KS is the sapwood-specific hydraulic conductivity
175 (mol m–1s–1 MPa–1); AS/AL is the ratio of sapwood to leaf area (m2m–2) $\Delta\Psi max$ is the

maximum decrease in water potential from soil to leaves (MPa) h is the transpiration stream pathlength (m), roughly equivalent to plant height, and E is the transpiration rate (mol m–2s–1),

Combining the above two equations we obtain a link between water transportation and photosynthesis:

$$Ks\ \Delta\Psi max\ AS/AL\ /\ h = 1.6\ VPD\ A_{area} / (ca - ci) /Patm = E \quad (3)$$

Note that here we focus on forest-stand scale as an average across time. Relationships could be very different at other scales (Mencuccini *et al.*, 2019a).

In drier sites with higher VPD, despite less open stomata (less gs and less ci), there should inevitably be a larger E (Granier *et al.*, 1996) and more negative ΔΨmax (Gleason *et al.*, 2013); therefore smaller maximum tree height, and more negative turgor loss point (TLP, Mpa) in drier sites to increase hydraulic resistance (note that TLP must be more negative than ΔΨmax) (Ryan & Yoder, 1997; Bartlett *et al.*, 2012). Equation 3 implies that in drier sites with high VPD, plants require a larger AS/AL and/or larger Ks in order to support the same amount of photosynthesis with enhanced transpiration. Following the xylem safety–efficiency trade-off (Manzoni *et al.*, 2013; Gleason *et al.*, 2016; Bittencourt *et al.*, 2016; Grossiord *et al.*, 2020b) (although arguments against this trade-off exist, here we present testable hypotheses expected by the trade-off), plants at drier sites would be expected to have lower hydraulic efficiency and lower hydraulic conductivity. Lower hydraulic conductivity is often associated with smaller vessel diameter, higher vessel density and higher wood density (Poorter *et al.*, 2010; Schuldt *et al.*, 2013; Hoeber *et al.*, 2014). Such patterns have been observed along an Australian aridity gradient (Gleason *et al.*, 2013; Pfautsch *et al.*, 2016), but no effect of aridity on vessel diameter was reported (Olson & Rosell, 2013; Olson *et al.*, 2014). Plants in drier sites should have increased hydraulic safety - more negative TLP and more negative P50 (Hacke *et al.*, 2001; Martínez-Vilalta *et al.*, 2009; Gleason *et al.*, 2013; Togashi *et al.*, 2015; Liu *et al.*, 2019; López *et al.*, 2021). In short, toward drier sites, we would expect to see, higher AS/AL and more negative TLP. The safety-efficiency trade-off implies lower Ks, smaller vessel diameter, higher vessel density and higher wood density.

The trade-off between Ks and AS/AL is also embedded in the variance of traits in equation 3. Ks and AS/AL could vary by two orders of magnitude (100-fold variation) (Mencuccini *et al.*, 2019b) on a global scale, while ci/ca and A_{area} vary much less (ci/ca: 2 fold; A_{area}: 10 fold) (Wright *et al.*, 2004; Wang *et al.*, 2017b). This leads to a trade-off between Ks and AS/AL (i.e. KS x AS/AL should vary less than either of them). However, given that there are also variations of ci/ca, A_{area}, h and $\Delta\Psi max$, it is possible that different species range along a spectrum from high A_{area} and E to low A_{area} and E while always satisfying equation 3 (Prentice *et al.*, 2014).

In short, the above review leads to an integrated hypothesis that plants in drier (normally also brighter) sites tend to develop a photosynthesis strategy with less stomatal conductance and hence lower ci, stronger photosynthetic capacities (larger V_{cmax25}, J_{max25} and A_{area}) with more maintenance cost (higher Rd and Rs), higher maximum carbon assimilation rate and larger maximum evapotranspiration which the water transport system would adjust to with higher AS/AL, lower Ks, lower tree height and more negative TLP. Information on leaf economic traits is provided in Appendix 3. We break the above prediction down into 16 testable hypotheses (Table 1) and test each of them along a forest aridity gradient.

Materials and Methods

Study sites - the aridity gradient

This study presents and analyses physiological traits data collected from seven one-hectare forest and savanna plots distributed along a wet to dry rainfall gradient across three sites, Ankasa (ANK, moist rainforest), Bobiri (BOB, semi-deciduous forest) and Kogyae (KOG, dry forest and mesic savanna), in Ghana, West Africa (Figure S1 S2) (Moore *et al.*, 2018; Oliveras *et al.*, 2020), as part of the Global Ecosystem Monitoring (GEM) network (Malhi *et al.*, 2021). These sites share very similar mean annual temperature but span a steep gradient of aridity (Figure 1), which provided a "natural laboratory" to disentangle the hydraulic aspect of plant traits variation from temperature.

Although one-hectare plots (e.g. BOB-02) within the same site (e.g. BOB) share very similar air temperature and precipitation, they can differ in terms of soil moisture supply due to small-scale variations in soil properties and topography (Table S1). Along the aridity gradient, there are also variations in soil and vegetation type, with vegetation seasonality and deciduousness increasing considerably towards drier sites (Moore *et al.*, 2018). More information about the soil properties and climate of all three sites can be found in (Domingues *et al.*, 2010; Chiti *et al.*, 2010; Moore *et al.*, 2018). Moreover, the swampy rainforest (ANK03) is partly inundated during the wet season unlike ANK01, which is located on a hill and never inundated. From KOG02 (dry forest), KOG04 to KOG05 (savanna), forest plots become more deciduous with a smaller number of trees. Within any site, there are many common species between plots but species composition (e.g., top five abundant species) could still be very different. There is almost no common abundant species between the three sites (ANK, BOB and KOG).

Aridity index and soil moisture stress

At site scales, we calculated an aridity index as the ratio of annual potential evapotranspiration (PET) to mean annual precipitation (MAP). To understand soil moisture stress experienced by plants, we reported not only measured surface (12 cm depth) soil volumetric water content, but also hydraulic simulations on plot scales with SPLASH v2.0 (Sandoval & Prentice, 2020). This model requires three sets of input data: (1) field observed climate data at site scale during 2011-2016 (2) soil properties measured following the RAINFOR protocols (Quesada *et al.*, 2010); (3) terrain data: root zone was assumed 2m, while upslope drainage area, slope inclination and orientation were extracted from (Yamazaki *et al.*, 2019). We considered two modelled indices: the relative soil moisture saturation (Θ) was defined as the volumetric water content (θ) normalized by the volumetric water content at saturation (θ_{SAT}); a vegetation water stress index (α) was estimated as the ratio of annual actual evapotranspiration (AET) to PET.

Functional trait data measurements

Leaf traits field campaigns to measure leaf traits were conducted using a standardized protocol between October 2015 and September 2016 in all plots (Oliveras *et al.*, 2020), covering both dry and wet seasons (see Appendix 1 for sampling protocol). To ensure consistent comparison along the aridity gradient, only sun leaves were sampled. Sampled leaves were chosen from individuals that correspond to the most dominant species in each plot. To determine the target species, species contributing to up to 80% of the total basal area of the plot were ranked by basal area. As equation 3 focuses on daytime conditions with maximum transpiration, we use Kp (potential specific hydraulic conductivity) as a proxy of Ks and plant stature (H_{max}) as a proxy of path length (h). Kp was calculated from vessel density and vessel diameter following (Poorter *et al.*, 2010).

Following (Prentice *et al.*, 2014), we calculated stem respiration per leaf area (Rs_leaf) instead of the commonly presented Rs_stem, as a 'maintenance cost of photosynthesis' (See Appendix 1). To our knowledge, Rs_leaf has not previously been presented with in-situ data in the literature. Here we argue the importance to understand stem respiration from per leaf area perspectives because (1) higher stem respiration per stem area has been found in wetter sites (Yang *et al.*, 2016), contradictory to theoretical expectation (Prentice *et al.*, 2014) (2) consistency with photosynthetic traits which were commonly reported per leaf area.

All data reported in this study were field-measured except for wood density, which was obtained from a global species database (Zanne *et al.*, 2009). Global scale sapwood-to-leaf-area ratio in Figure 3 is sourced from (Mencuccini *et al.*, 2019b). Global scale vessel diameter in Figure S4 is sourced from (Choat *et al.*, 2012).

Statistical analysis

Hypotheses 1-14 (Table 1) were tested by significant differences between wet and dry sites. Principal component analysis (PCA) and standardized major axis regression are used to understand the relationship between Ks, As/AL and photosynthesis traits (Hypothesis 15-16).

We performed a plot-to-plot comparison in answering Hypotheses 1 to 14 as follows: (1) The distribution was visually inspected with histograms and transformations were applied if necessary.

(2) Outliers were checked with the R package *outliers::scores*, 'iqr' method with threshold 1.5. This removed leaves/trees with extreme values but made the community-weighted mean a better representation of the whole plot. (3) Community-weighted means were calculated based on the basal area of each species. Standard error was calculated with the same weights (Madansky & Alexander, 2017). (4) Significance of differences in plot-to-plot community-weighted means were then tested with *lm*(), *glht*(), and *cld*(). (See Rscript *community_weighted_mean_Ghana_log_YS.R* for a full description). In testing Hypotheses 1-14, a hypothesis was accepted if KOG (dry region) was significantly different to ANK (wet region) while BOB (middle aridity) sat in between (Figure 1). (5) Variance partitioning was done with *vegan::varpart()*, following the 'RDA' method with the expression: *varpart* (Trait, ~ Plot, ~ Species, data = Trait). Variance partitioning reveals whether the change of traits along the aridity gradient was driven by intraspecific or interspecific variation. Variance partitioning is also used to diagnose whether the intra-specific variation or measurement errors are overwhelming. To double-check the impact of intraspecific variation, we recalculated a community-weighted mean by assuming that the same species share the same value of trait (i.e. remove intraspecific variation) and extrapolated traits value to forest plots without trait measurements (Appendix 5)

For hypothesis 16, we applied Principal Component Analysis (PCA) with *FactoMineR::PCA*(), (See Rscript ~/link_hydraulic_photosynthesis/PCA.R). Asat, Kp, AS/AL and V_{cmax25} were log10 transformed. We avoid standardization by setting 'scale.unit' as False in function PCA() so that the variance of a trait was reflected by the length of an arrow in Figure 2. Trait-trait correlations (bivariate plot) were calculated (Rscript *Compare_with_Others.R*). For hypothesis 15, the slopes and significance of correlation were calculated using Standard Major Axis Regression (*function smatr::sma*()), which is preferable to ordinary least squares regression in summarizing the relationship between two plant traits (Wright *et al.*, 2005; Warton *et al.*, 2012) as it considers uncertainties of both axes. All analyses were done at the species level (i.e. each point in Figure 2 represents a species) to compare with other studies and join among datasets. Hypothesis 15 was also tested at the global scale because Ks was reported to negatively correlate with AS/AL but there is no report on the global correlation between Kp and AS/AL (Appendix 4).

Results

Aridity gradient

The values of the aridity index (PET/MAP) (site scale) revealed a clear aridity gradient from ANK (moist rainforest site) to BOB (mid) and KOG (dry) (Appendix 2). The same order could be arrived at with VPD or maximum cumulative water deficit (MCWD). The standard deviation of monthly VPD also suggested that the seasonality was weaker in ANK and increased towards KOG.

On the other hand, the simulations of relative soil moisture saturation (Θ) and vegetation water stress index (α) (plot scale) showed that BOB was the least soil moisture stressed site, followed by ANK and KOG. BOB-02 had the highest values in these two metrics. The model reported the highest runoff at ANK-03, capturing to some degree the seasonal flooding, as also observed in the field. The different patterns of Θ (or α) to aridity index along the aridity gradient were caused by the soil characteristics which in turn define water holding capacity (WHC) and hydraulic conductivity; for example, the plots in BOB were atmospherically drier (higher PET/MAP) than in ANK but they could hold more water (higher Θ). Especially in BOB-02, the infiltration rate was strongly reduced (60 mm/hr, less than half of ANK plots), and hence water can stay more time in the root zone while percolating. This acts as a buffer against the evaporative demand, maintaining water availability during dry months. The hydrological modelling outputs also matched with field observation of plot vegetation characteristics (see Methods).

For presentation (Figure 1), we rank sites by aridity index and then plots within sites by soil moisture stress.

The effect of aridity on traits

From a photosynthesis perspective, along the aridity gradient, we saw consistency between theoretical prediction and field measurements (Table 1) for all traits: ci/ca (0.71 to 0.85), V_{cmax25}

(21.58 to 46.48 umol CO_2 m2 s-1), J_{max25} (38.48 to 91.44 umol CO_2 m2 s-1), Rd (-1.66 to -2.41 umol CO_2 m2 s-1), Rs (3.76 to 11.70 umol CO_2 m2 s-1), Asat (4.56 to 7.72 umol CO_2 m2 s-1) and Amax (15.88 to 22.86 umol CO_2 m2 s-1). However, we saw less consistency between theory and field measurements regarding leaf economic traits (Appendix 3). Nmass was expected to increase from wet to dry but this is not backed by our field measurements. LMA was slightly higher in the dry sites than in the wet sites as theoretically expected, but not a gradual increase. Pmass increased gradually from wet to dry plots, (from 0.94 to 1.67 g kg-1) along the gradient in accord with global observation. Although the link among soil nitrogen, leaf nitrogen and photosynthesis was frequently made (Walker *et al.*, 2014; Gvozdevaite *et al.*, 2018), we found that such a link is rather ambiguous along the aridity gradient on site scale.

From a water transpiration perspective, the hypotheses were consistent with field measurements for leaf traits. AS/AL was higher in drier sites (359.62 to 901.66 cm2 m-2) and TLP was more negative in drier sites (-1.33 to -1.63 Mpa). However, no consistency was found between theoretical expectations and field measurements for any xylem-related traits. Along the aridity gradient, there was an increasing trend of field Kp toward drier sites (from 28.62 to 59.29 kg m-1 Mpa-1 s-1), against the xylem safety-efficiency trade-off. Behind the above trend, vessel diameter and vessel density also contradicted the hypotheses. Vessel diameter did not change along the aridity gradient, while vessel density increased toward drier sites (from 49.14 to 82.07 micron). The drier sites (KOG) had higher Kp, higher twig density and higher wood density than the wetter sites on site scales, but we also found Kp negatively correlated with twig density on species scales (see Appendix 4). ANK-01 had very high wood density and twig density which breaks the increasing trend formed by other plots. To conclude, the trends of all photosynthetic traits were successfully predicted by theories based on VPD alone. As leaf economy traits, soil nutrients and soil moisture (Θ or α) overall did not have a clear trend along the gradient, considering nutrient and water deliveries to leaves does not seem to aid the prediction of variation of photosynthetic traits along the aridity gradient.

With variance partitioning, we found that the plot-to-plot trends of all traits were dominated by inter-specific rather than intra-specific variation (i.e., components [a] are smaller than [b] in Appendix 5). Such a finding was expected as there are few common species between plots. The

361 analogous patterns between twig and wood density along the aridity gradient also supported
362 species turnover since twig density was field measured and wood density was parsed from a global
363 database by species (Zanne *et al.*, 2009). To double-check the conclusion of predominant
364 interspecific variation, we recalculated community weighted means by assuming that the same
365 species share the same value of trait (i.e. remove intraspecific variation) and extrapolated trait
366 values to forest plots without trait measurements. We found that the conclusions in Table 1 still
367 hold after extrapolation (Appendix 5). The trend of trait variation from plot to plot could be well
368 re-constructed on a species basis, which hints at the possibility of extrapolation to other sites with
369 species composition information or upscaling to larger scales. Nonetheless, for within plot
370 variance, intraspecific variation or measurement errors (component [d]) were large for most traits:
371 accounting for 95% of turgor loss point variance, followed by V_{cmax25} (74%) and J_{max25} (66%).

372

373 ### The coordination between photosynthesis and water transportation

374 Data from our West African aridity gradient reveal a weak positive correlation between Kp and
375 AS/AL, contradictory toHypothesis 15, and inconsistent with the negative correlation that emerged
376 on global scales (Appendix 4). AS/AL for the Ghanaian aridity gradient was higher than the
377 pantropical average (Appendix 4). For hypothesis 16, we further explore the link between AS/AL,
378 Kp and photosynthetic trait using PCA. Species with both high AS/AL and Kp tend to have higher
379 V_{cmax25} and lower ci/ca. Such species tend to be deciduous and appear more in drier plots (Figure
380 2). There was a larger variance of hydraulic traits compared to photosynthetic traits (Figure 2).
381 The pattern is consistent if we redo the above PCA with Asat instead of V_{cmax25} (Appendix 4). This
382 finding supports hypothesis 16 (Table 1) as well as equation 3.

383 ## Discussion

384 ### The trend of traits along the aridity gradient

385 Although most hypotheses (Table 1) have been tested with spatially varying aridity at multiple
386 scales (Harrison *et al.*, 2021), testing them along the Ghana aridity gradient helps to scrutinize the

pattern in the absence of temperature variation. The patterns of all photosynthetic traits measured along the aridity gradient (ci/ca, J_{max25}, V_{cmax25}, Dresp, Rs, Asat, Amax, namely hypotheses 1-7) are consistent with the theoretical expectations, which underscores that aridity is a direct and critical driver of photosynthetic traits, in absence of confounding effect with temperature. The increase of photosynthetic capacity towards drier sites is useful in explaining multiple previous observations, including that (1) savanna has higher photosynthesis rates than wet evergreen forest (Gvozdevaite, 2018; Oliveras *et al.*, 2020) (2) woody savanna has sparse canopy but similar net primary productivity to wet evergreen forest (Moore *et al.*, 2018) (3) for wet Amazonia forests, leaves flushed in dry season have higher photosynthetic capacities which increase forest productivity (Wu *et al.*, 2020; Green *et al.*, 2020).

From a water transportation perspective, forests in drier sites have higher TLP, lower H_{max} and higher AS/AL (agreed with hypotheses 8-10), in support of a greater mid-day transpiration stream. However, hypotheses derived from the safety-efficiency trade-off (hypotheses for Kp and vessel diameter) were not in agreement with measurements along the aridity gradient. It is possible that the trade-off may work well for single-species studies (Pritzkow *et al.*, 2020) and become weak on large scales and across species (Gleason *et al.*, 2016; Grossiord *et al.*, 2020b). Much higher deciduousness in KOG (dry site) than in the wet sites may play a role as higher hydraulic efficiency was reported from deciduous species or more deciduous forests (Choat *et al.*, 2005; Chen *et al.*, 2008; Liu *et al.*, 2021). We reported a negative correlation between AS/AL and Kp at global scales but a positive correlation along the aridity gradient (Appendix 4). One of the reasons for these contrasting opposite correlations may lie in a geographical sampling bias – the global dataset with scarce data points from West Africa compared with the Ghanaian dataset. The other possibility could be a confounding effect by temperature or vegetation type at the global scale (a Simpson's paradox); for example, a negative correlation between AS/AL and Ks was reported globally (Mencuccini *et al.*, 2019b) and on continental (Australia) scales (Gleason *et al.*, 2012), but an insignificant correlation was also reported for tropical forest stands on local scales without varying temperature (Poorter *et al.*, 2010; Schuldt *et al.*, 2013; Hoeber *et al.*, 2014).

By assuming that traits with a clear and strong trend along the aridity gradient are more tightly bound with aridity (Figure 1), ci/ca, TLP and AS/AL was found to be the most aridity-driven traits.

The runners-up are Rd, Rs, $J_{max25,}$ and V_{cmax25}, which was thought acclimated to ci/ca and light intensity (Wang *et al.*, 2017b). Although ci/ca, Vcmax25, Kp and AS/AL all vary from wet to dry sites, the PCA (Figure 2) further illustrates that, surprisingly, it is photosynthetic traits instead of hydraulic traits that contrast species from wet to dry sites (also from evergreen to deciduous). Given that large photosynthetic traits variation from wet to dry plot was induced by species turnover (Appendix 5), our studies hint that facing a drier climate, if allowed time, West African forests photosynthesis could adapt to a drier climate by changing species abundance with possibly more deciduousness and higher photosynthesis capacity albeit less stomatal openness (Aguirre-Gutiérrez *et al.*, 2019). Without consideration of the positive effect of aridity on photosynthetic capacity, models could possibly underestimate forest productivity under future drier climates.

Combining photosynthesis and hydraulic hypotheses

Our analysis unifies photosynthesis and hydraulic hypotheses to explain plant strategies along the aridity gradient. Namely, species in drier sites (with more deciduousness) tend to develop a photosynthesis strategy with less stomata openness (ci/ca), stronger photosynthetic capacities (J_{max25} and V_{cmax25}) with more maintenance cost (higher Rd and Rs), quicker photosynthesis rate (Asat) and larger maximum transpiration, supported by large Kp and large AS/AL. The product of AS/AL and Kp is a proxy of water delivery per leaf area, which was previously found well correlated with proxies of photosynthesis rate: Asat (Santiago *et al.*, 2004), quantum yield of electron transport (Brodribb & Feild, 2000) and electron transfer rate (Brodribb *et al.*, 2002). The large variance of wood traits (way larger than leaf traits) (Mencuccini *et al.*, 2019b), hints that plants might have a wide range of choices of traits combinations to provide adequate water transportation (Sperry *et al.*, 2002; Prentice *et al.*, 2014) in drier sites to support faster photosynthesis. Further investigations into xylem functioning are required to understand how larger water transportation was achieved in drier sites. Notably, we successfully predicted plants photosynthesis strategies along the aridity gradient (hypothesis 1-7) based solely on VPD without incorporating leaf economic traits nor soil moisture. Nonetheless, our theoretical deduction implicitly assumes that plants in the drier site could arrange water transportation (e.g., high AS/AL and high Kp in Figure 2) and have adequate access to belowground water. Regarding the ongoing discussion on the impact of VPD versus soil moisture, soil moisture may be playing a role at other

445 temporal scales (e.g., daily) (Liu *et al.*, 2020; Fu *et al.*, 2022) or under extreme soil drought (Sperry
446 *et al.*, 2002).

447 Conclusion

448 Along the aridity gradient, we found that species with both higher AS/AL and Kp (greater potential
449 mid-day transpiration steam) tend to have higher Vcmax25 and lower ci/ca, which appears more
450 in drier sites with more deciduous species. With such a working example in West Africa, the study
451 not only underscores the importance of incorporating the positive effect of aridity on
452 photosynthesis capacity in carbon modelling but also simplifies the coupling between carbon and
453 water cycle: future modelling studies, following our theoretical framework, could estimate site-
454 time-averaged leaf-level photosynthesis simply from VPD only and consider soil moisture (or
455 water availability) in simulating forest stands dynamic such as drought-induced mortality or
456 seasonality (Hubau *et al.*, 2020; Bauman *et al.*, 2022).

457 Data availability

458 Figures could be downloaded from

459 https://github.com/Hzhang-ouce/Ghana_rainfall_trait_variation_optimality_github. To reproduce
460 figures, data and R codes mentioned in the main text could also be found in the above repository.

461

462

463 Acknowledgements

464 We thank Natascha Luijken, Ya-Jun Chen, Yu-Heng Sun, Maurizio Mencuccini and Akwasi
465 DGyamfi, Guillaume Delhaye for valuable discussion and assistance with data processing. Y.M.
466 is supported by the Jackson Foundation. H.Z. received Henfrey Scholarship (by St Catherine's
467 College, Oxford) and Tang Scholarship (by China-Oxford Schorlarship Fund). The field data
468 collection was funded by a grant award (ERC GEM-TRAIT, grant no. ERC-2012-ADG_20120216)
469 to Y.M., with additional support for the fieldwork from a Royal Society-Leverhulme Africa

Capacity Building Award and Marie Curie Fellowship to I.O. (FP7-2012-IEF-327990-TipTropTrans).

Conflict of interest

The authors have no conflicts of interest to declare that are relevant to the content of this article.

Author contributions

IO, YM, ICP, and HZ designed the research and interpreted the results. DS did the hydraulic modelling. YM, AG, TP, MB, KZ, SAB, JAG, IO, HZ contributed to data collection. HZ carried out the analyses and wrote the paper with inputs and revisions from all co-authors.

Table 1 Traits name, unit, hypotheses and findings from field measurements along the rainfall gradient, Green color denotes consistency between theory and our field data. Orange color denote inconsistency.

#	Hypotheses	Data	Consistent
	Variables associated with photosynthesis and respiration (Optimality theory)		
1	Toward drier sites, the ratio between leaf-internal and ambient CO2 (ci/ca, %) (from 13C) **decreases**.	Decrease	✓
2	Toward drier sites, Rubisco carboxylation capacity at 25 C° (Vc_{max25}, umol CO2 m2 s-1) **increases**.	Slight increase	✓
3	Toward drier sites, electron transport capacity at 25 C° (J_{max25}, umol CO2 m2 s-1) **increases**.	Slight increase	✓
4	Toward drier sites, light saturated assimilation rate at 400 ppm (Asat, umol CO2 m2 s-1) **increases**.	Increases	✓
5	Toward drier sites, light saturated assimilation rate at 2000 ppm (Amax, umol CO2 m2 s-1) **increases.**	Increase	✓

6	Toward drier sites, leaf dark respiration (Rd, umol CO2 m2 s-1) **increases**.	Increase	✓
7	Toward drier sites, specific stem respiration (Rs, umol CO2 m2 s-1) **increases.**	Increase	✓
	Variables associated with water transportation		
8	Toward drier sites, Sapwood to leaf area ratio (Huber value) (AS/AL, cm2 m-2) **increases.**	Increase	✓
9	Toward drier sites, turgor loss point (TLP, MPa) becomes more negative.	More negative	✓
10	Toward drier sites, plant stature, calculated as maximum tree height of a species (H_{max}, m) **decreases**.	Slight decrease	✓
11	Toward drier sites, wood density (g cm-3) and twig density (g cm-3) **increase** (if following the safety-efficiency trade-off).	Slight increase	✓
12	Toward drier sites, potential specific hydraulic conductivity (Kp, kg m-1 Mpa-1 s-1) **decreases** (if following the safety-efficiency trade-off).	Slight increase	
13	Toward drier sites, vessel diameter (micron) **decreases.** (if following the safety-efficiency trade-off).	No trend	
14	Toward drier sites, vessel density (mm-2) **decreases.** (if following the safety-efficiency trade-off).	Increase	
15	AS/AL and Kp are negatively correlated. (if following safety-efficiency trade-off, and global scale analysis – see introduction)	Positive correlation	
16	For species with high A_S/A_L and Kp, there is high Vcmax (or high Asat)	See Figure 3	✓

'Data' column summarize patterns in Figure 1. A trend of trait is qualitatively recognized if KOG (dry region) is significantly different to ANK (wet region) while BOB ranks between. 'Slight increase' suggest that the pattern fits the above criteria broadly albeit one plot behave inconsistently. Colours indicate results that are consistent (green), weakly consistent (light green) and inconsistent (orange) with theoretical expections. Ticks in the column 'consistent' indicate consistency between hypothesies and data

485

MAT, MAP and soil moisture

486

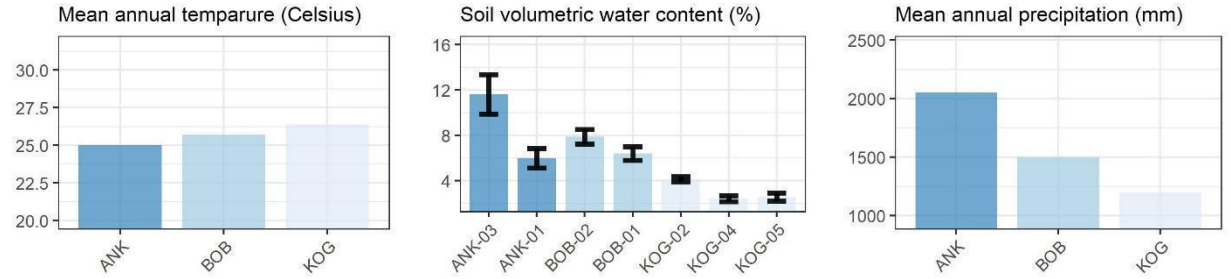

487

Variables associated with photosynthesis and respiration

488

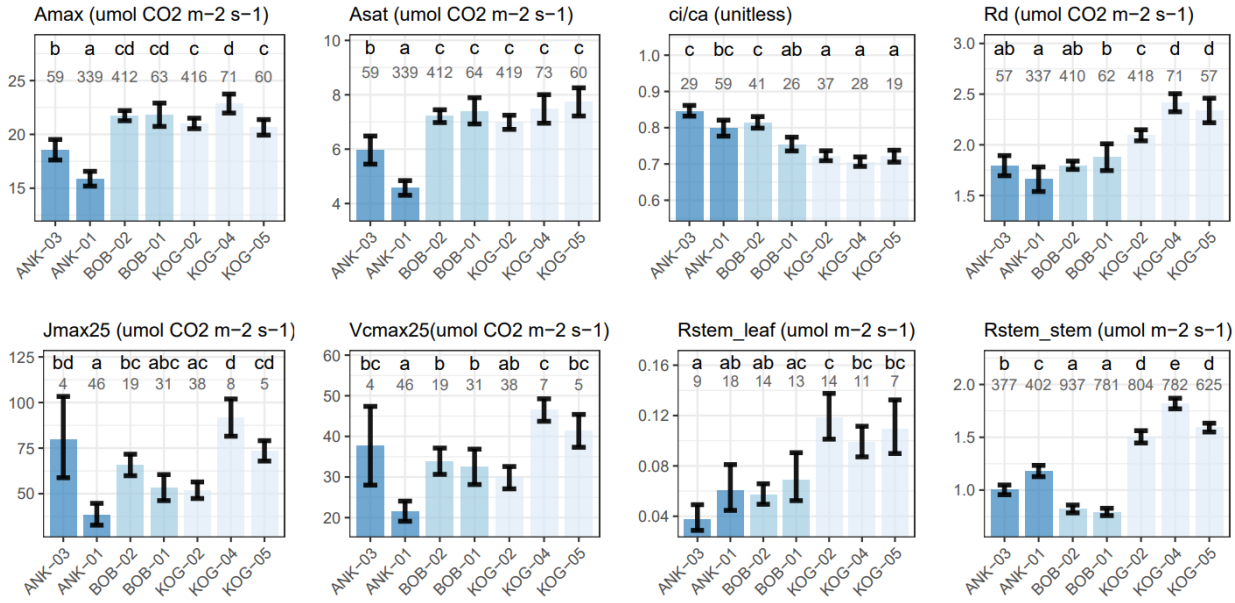

489

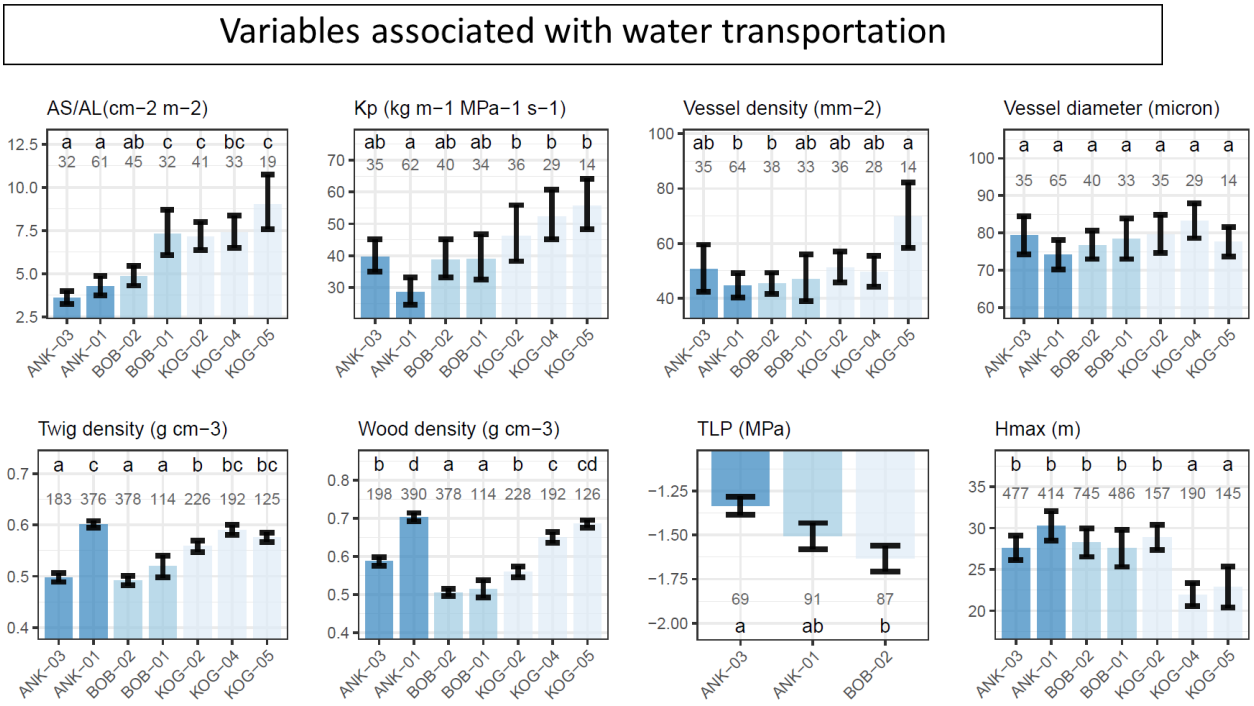

Figure 1 Plot scale community weighted mean (with standard error) from the wettest (left) to the driest (right) plot. Mean annual air temperature, precipitation and soil volumetric water content at 12 cm depth were also shown. Forest plots are arrayed from left to right in order of increasing aridity according to the aridity gradient description described in the text. The number denotes the number of samples, which could be a leaf, a branch, a tree or a species depending on the variable. The letters denote significance (P<0.05) in plot-to-plot difference.

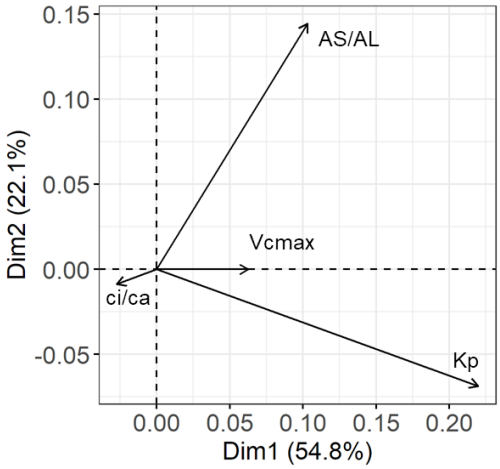

500

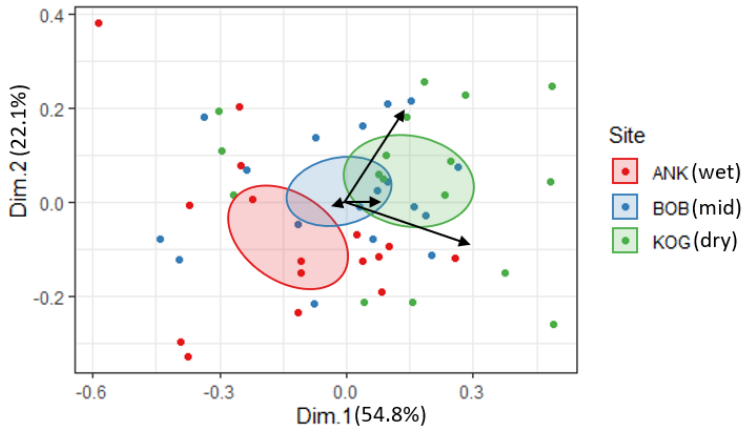

501

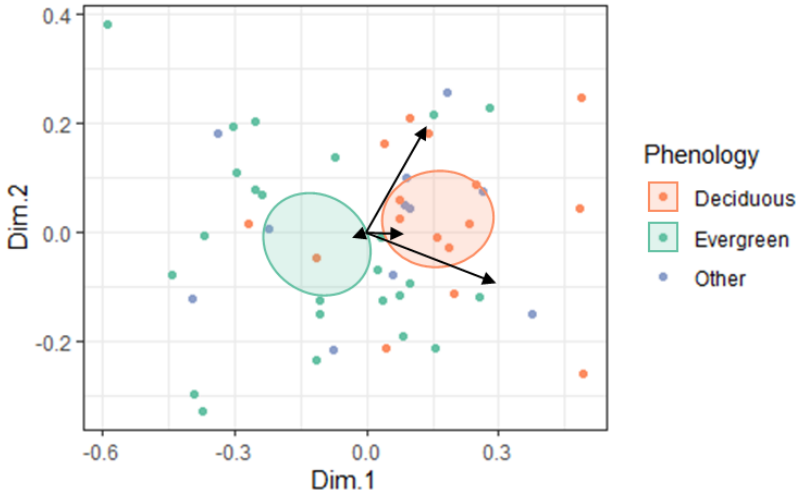

502

Figure 2 Principal components analysis for Huber value (AS/AL), the ratio between leaf internal and ambient CO_2 (ci/ca), Rubisco carboxylation capacity at 25 degree (Vcmax25) and potential specific conductivity (Kp) on species scale. Values are transformed to achieve normal distribution but not standardized to equal variance; therefore the length of arrows denotes the variance of the specific trait. The ellipses for each site are confidence ellipses around group mean points. The PCA axes in all figures are identical. Note that the three figures display the same PCA, but with a different classification of scatter points.

References

Aguirre-Gutiérrez J, Oliveras I, Rifai S, Fauset S, Adu-Bredu S, Affum-Baffoe K, Baker TR, Feldpausch TR, Gvozdevaite A, Hubau W, *et al.* 2019. Drier tropical forests are susceptible to functional changes in response to a long-term drought. *Ecology Letters* **22**: 855–865.

Atkin OK, Bloomfield KJ, Reich PB, Tjoelker MG, Asner GP, Bonal D, Bönisch G, Bradford MG, Cernusak LA, Cosio EG, *et al.* 2015. Global variability in leaf respiration in relation to climate, plant functional types and leaf traits. *New Phytologist* **206**: 614–636.

Bahar NHA, Ishida FY, Weerasinghe LK, Guerrieri R, O'Sullivan OS, Bloomfield KJ, Asner GP, Martin RE, Lloyd J, Malhi Y, *et al.* 2017. Leaf-level photosynthetic capacity in lowland Amazonian and high-elevation Andean tropical moist forests of Peru. *New Phytologist* **214**: 1002–1018.

Bartlett MK, Scoffoni C, Sack L. 2012. The determinants of leaf turgor loss point and prediction of drought tolerance of species and biomes: A global meta-analysis. *Ecology Letters* **15**.

Bauman D, Fortunel C, Delhaye G, Malhi Y, Cernusak LA, Bentley LP, Rifai SW, Aguirre-Gutiérrez J, Menor IO, Phillips OL, *et al.* 2022. Tropical tree mortality has increased with rising atmospheric water stress. *Nature*.

Beerling DJ, Quick WP. **1995**. A new technique for estimating rates of carboxylation and electron transport in leaves of C3 plants for use in dynamic global vegetation models. *Global Change Biology* **1**: 289–294.

Bittencourt PRL, Pereira L, Oliveira RS. **2016**. On xylem hydraulic efficiencies, wood space-use and the safety–efficiency tradeoff. *New Phytologist* **211**: 1152–1155.

Björkman O. **1981**. Responses to Different Quantum Flux Densities. *Physiological Plant Ecology I*: 57–107.

Brodribb TJ, Feild TS. **2000**. Stem hydraulic supply is linked to leaf photosynthetic capacity: evidence from New Caledonian and Tasmanian rainforests. *Plant, Cell & Environment* **23**: 1381–1388.

Brodribb TJ, Holbrook NM, Gutierrez M v. **2002**. Hydraulic and photosynthetic co-ordination in seasonally dry tropical forest trees. *Plant, Cell & Environment* **25**: 1435–1444.

Canadell JG, Monteiro PMS, Costa MH, Cunha LC da, Cox PM, Eliseev A v., Henson S, Ishii M, Jaccard S, Koven C, *et al.* 2021. Global carbon and other biogeochemical cycles and feedbacks. In: Climate Change 2021: The Physical Science Basis. Contribution of Working Group I to the Sixth Assessment Report of the Intergovernmental Panel on Climate Change.

Chen J-W, Zhang Q, Cao K-F. **2008**. Inter-species variation of photosynthetic and xylem hydraulic traits in the deciduous and evergreen Euphorbiaceae tree species from a seasonally tropical forest in south-western China. *Ecological Research* **24**: 65.

Chiti T, Certini G, Grieco E, Valentini R. **2010**. The role of soil in storing carbon in tropical rainforests: The case of Ankasa Park, Ghana. *Plant and Soil* **331**: 453–461.

Choat B, Ball MC, Luly JG, Holtum JAM. **2005**. Hydraulic architecture of deciduous and evergreen dry rainforest tree species from north-eastern Australia. *Trees* **19**: 305–311.

Choat B, Jansen S, Brodribb TJ, Cochard H, Delzon S, Bhaskar R, Bucci SJ, Feild TS, Gleason SM, Hacke UG, *et al.* 2012. Global convergence in the vulnerability of forests to drought. *Nature 2012 491:7426* **491**: 752–755.

553 **Cunningham SC**. **2005**. Photosynthetic responses to vapour pressure deficit in temperate and
554 tropical evergreen rainforest trees of Australia. *Oecologia* **142**: 521–528.

555 **Dai Z, Edwards GE, Ku MSB**. **1992**. Control of photosynthesis and stomatal conductance in
556 Ricinus communis L.(castor bean) by leaf to air vapor pressure deficit. *Plant physiology* **99**: 1426.

557 **Domingues TF, Meir P, Feldpausch TR, Saiz G, Veenendaal EM, Schrodt F, Bird M,**
558 **Djagbletey G, Hien F, Compaore H, *et al.* 2010**. Co-limitation of photosynthetic capacity by
559 nitrogen and phosphorus in West Africa woodlands. *Plant, Cell & Environment* **33**: 959–980.

560 **Franklin O, Harrison SP, Dewar R, Farrior CE, Brännström Å, Dieckmann U, Pietsch S,**
561 **Falster D, Cramer W, Loreau M, *et al.* 2020**. Organizing principles for vegetation dynamics.
562 *Nature Plants* **6**: 444–453.

563 **Fu Z, Ciais P, Prentice IC, Gentine P, Makowski D, Bastos A, Luo X, Green JK, Stoy PC,**
564 **Yang H, *et al.* 2022**. Atmospheric dryness reduces photosynthesis along a large range of soil water
565 deficits. *Nature Communications 2022 13:1* **13**: 1–10.

566 **Gleason SM, Butler DW, Waryszak P**. **2013**. Shifts in leaf and stem hydraulic traits across aridity
567 gradients in eastern Australia. *International Journal of Plant Sciences* **174**: 1292–1301.

568 **Gleason SM, Butler DW, Ziemińska K, Waryszak P, Westoby M**. **2012**. Stem xylem
569 conductivity is key to plant water balance across Australian angiosperm species. *Functional*
570 *Ecology* **26**: 343–352.

571 **Gleason SM, Westoby M, Jansen S, Choat B, Hacke UG, Pratt RB, Bhaskar R, Brodribb TJ,**
572 **Bucci SJ, Cao KF, *et al.* 2016**. Weak tradeoff between xylem safety and xylem-specific hydraulic
573 efficiency across the world's woody plant species. *New Phytologist* **209**: 123–136.

574 **Granier A, Hue R, Barigah ST**. **1996**. Transpiration of natural rain forest and its dependence on
575 climatic factors. *Agricultural and Forest Meteorology* **78**: 19–29.

576 **Green JK, Berry J, Ciais P, Zhang Y, Gentine P**. **2020**. Amazon rainforest photosynthesis
577 increases in response to atmospheric dryness. *Science Advances* **6**.

Grossiord C, Buckley TN, Cernusak LA, Novick KA, Poulter B, Siegwolf RTW, Sperry JS, McDowell NG. **2020a**. Plant responses to rising vapor pressure deficit. *New Phytologist* **226**: 1550–1566.

Grossiord C, Ulrich DEM, Vilagrosa A. **2020b**. Controls of the hydraulic safety–efficiency trade-off. *Tree Physiology* **40**: 573–576.

Gvozdevaite A. **2018**. The role of economic, venation and morphological leaf traits in plant and ecosystem function along forest-savanna gradients in the tropics.

Gvozdevaite A, Oliveras I, Domingues TF, Peprah T, Boakye M, Afriyie L, da Silva Peixoto K, de Farias J, Almeida de Oliveira E, Almeida Farias CC, *et al.* 2018. Leaf-level photosynthetic capacity dynamics in relation to soil and foliar nutrients along forest–savanna boundaries in Ghana and Brazil. *Tree Physiology* **38**: 1912–1925.

Hacke UG, Sperry JS, Pockman WT, Davis SD, McCulloh KA. **2001**. Trends in wood density and structure are linked to prevention of xylem implosion by negative pressure. *Oecologia 2000 126:4* **126**: 457–461.

Han T, Feng Q, Yu T, Yang X, Zhang X, Li K. **2022**. Characteristic of Stomatal Conductance and Optimal Stomatal Behaviour in an Arid Oasis of Northwestern China. *Sustainability 2022, Vol. 14, Page 968* **14**: 968.

Harrison SP, Cramer W, Franklin O, Prentice IC, Wang H, Brännström Å, de Boer H, Dieckmann U, Joshi J, Keenan TF, *et al.* 2021. Eco-evolutionary optimality as a means to improve vegetation and land-surface models. *New Phytologist* **231**: 2125–2141.

Hoeber S, Leuschner C, Köhler L, Arias-Aguilar D, Schuldt B. **2014**. The importance of hydraulic conductivity and wood density to growth performance in eight tree species from a tropical semi-dry climate. *Forest Ecology and Management* **330**: 126–136.

Hubau W, Lewis SL, Phillips OL, Affum-Baffoe K, Beeckman H, Cuní-Sanchez A, Daniels AK, Ewango CEN, Fauset S, Mukinzi JM. **2020**. Asynchronous carbon sink saturation in African and Amazonian tropical forests. *Nature* **579**: 80–87.

Liu H, Gleason SM, Hao G, Hua L, He P, Goldstein G, Ye Q. **2019**. Hydraulic traits are coordinated with maximum plant height at the global scale. *Science Advances* **5**: eaav1332.

Liu L, Gudmundsson L, Hauser M, Qin D, Li S, Seneviratne SI. **2020**. Soil moisture dominates dryness stress on ecosystem production globally. *Nature Communications* **11**: 4892.

Liu H, Ye Q, Gleason SM, He P, Yin D. **2021**. Weak tradeoff between xylem hydraulic efficiency and safety: climatic seasonality matters. *New Phytologist* **229**: 1440–1452.

Long SP, Woolhouse HW. **1978**. The responses of net photosynthesis to vapour pressure deficit and CO2 concentration in Spartina townsendii (sensu lato), a C4 species from a cool temperate climate. *Journal of Experimental Botany* **29**: 567–577.

López R, Cano FJ, Martin-Stpaul NK, Cochard H, Choat B. **2021**. Coordination of stem and leaf traits define different strategies to regulate water loss and tolerance ranges to aridity. *New Phytologist* **230**: 497–509.

Maire V, Martre P, Kattge J, Gastal F, Esser G, Fontaine S, Soussana J-F. **2012**. The coordination of leaf photosynthesis links C and N fluxes in C3 plant species. *PloS one* **7**: e38345.

Maire V, Wright IJ, Prentice IC, Batjes NH, Bhaskar R, van Bodegom PM, Cornwell WK, Ellsworth D, Niinemets Ü, Ordonez A. **2015**. Global effects of soil and climate on leaf photosynthetic traits and rates. *Global Ecology and Biogeography* **24**: 706–717.

Malhi Y, Girardin C, Metcalfe DB, Doughty CE, Aragão LEOC, Rifai SW, Oliveras I, Shenkin A, Aguirre-Gutiérrez J, Dahlsjö CAL, *et al.* 2021. The Global Ecosystems Monitoring network: Monitoring ecosystem productivity and carbon cycling across the tropics. *Biological Conservation* **253**: 108889.

Manzoni S, Vico G, Katul G, Palmroth S, Jackson RB, Porporato A. **2013**. Hydraulic limits on maximum plant transpiration and the emergence of the safety–efficiency trade-off. *New Phytologist* **198**: 169–178.

Martínez-Vilalta J, Cochard H, Mencuccini M, Sterck F, Herrero A, Korhonen JFJ, Llorens P, Nikinmaa E, Nolè A, Poyatos R, *et al.* 2009. Hydraulic adjustment of Scots pine across Europe. *The New phytologist* **184**: 353–364.

Medlyn BE, Duursma RA, Eamus D, Ellsworth DS, Prentice IC, Barton CVM, Crous KY, de Angelis P, Freeman M, Wingate L. 2011. Reconciling the optimal and empirical approaches to modelling stomatal conductance. *Global Change Biology* **17**: 2134–2144.

Mencuccini M, Manzoni S, Christoffersen B. 2019a. Modelling water fluxes in plants: from tissues to biosphere. *New Phytologist* **222**: 1207–1222.

Mencuccini M, Rosas T, Rowland L, Choat B, Cornelissen H, Jansen S, Kramer K, Lapenis A, Manzoni S, Niinemets Ü, *et al.* 2019b. Leaf economics and plant hydraulics drive leaf : wood area ratios. *New Phytologist* **224**: 1544–1556.

Moore S, Adu-Bredu S, Duah-Gyamfi A, Addo-Danso SD, Ibrahim F, Mbou AT, de Grandcourt A, Valentini R, Nicolini G, Djagbletey G, *et al.* 2018. Forest biomass, productivity and carbon cycling along a rainfall gradient in West Africa. *Global Change Biology* **24**: e496–e510.

Neelin JD, Münnich M, Su H, Meyerson JE, Holloway CE. 2006. Tropical drying trends in global warming models and observations. *Proceedings of the National Academy of Sciences* **103**: 6110–6115.

Ögren E. 1993. Convexity of the Photosynthetic Light-Response Curve in Relation to Intensity and Direction of Light during Growth. *Plant physiology* **101**: 1013–1019.

Oliveras I, Bentley L, Fyllas NM, Gvozdevaite A, Shenkin AF, Peprah T, Morandi P, Peixoto KS, Boakye M, Adu-Bredu S, *et al.* 2020. The Influence of Taxonomy and Environment on Leaf Trait Variation Along Tropical Abiotic Gradients. *Frontiers in Forests and Global Change* **3**: 18.

Olson ME, Anfodillo T, Rosell JA, Petit G, Crivellaro A, Isnard S, León-Gómez C, Alvarado-Cárdenas LO, Castorena M. 2014. Universal hydraulics of the flowering plants: vessel diameter scales with stem length across angiosperm lineages, habits and climates. *Ecology Letters* **17**: 988–997.

Olson ME, Rosell JA. **2013**. Vessel diameter–stem diameter scaling across woody angiosperms and the ecological causes of xylem vessel diameter variation. *New Phytologist* **197**: 1204–1213.

Peng Y, Bloomfield KJ, Cernusak LA, Domingues TF, Colin Prentice I. **2021**. Global climate and nutrient controls of photosynthetic capacity. *Communications Biology 2021 4:1* **4**: 1–9.

Pfautsch S, Harbusch M, Wesolowski A, Smith R, Macfarlane C, Tjoelker MG, Reich PB, Adams MA. **2016**. Climate determines vascular traits in the ecologically diverse genus Eucalyptus. *Ecology Letters* **19**: 240–248.

Poorter L, McDonald I, Alarcón A, Fichtler E, Licona JC, Peña-Claros M, Sterck F, Villegas Z, Sass-Klaassen U. **2010**. The importance of wood traits and hydraulic conductance for the performance and life history strategies of 42 rainforest tree species. *New Phytologist*.

Prentice IC, Dong N, Gleason SM, Maire V, Wright IJ. **2014**. Balancing the costs of carbon gain and water transport: testing a new theoretical framework for plant functional ecology. *Ecology Letters* **17**: 82–91.

Pritzkow C, Williamson V, Szota C, Trouvé R, Arndt SK. **2020**. Phenotypic plasticity and genetic adaptation of functional traits influences intra-specific variation in hydraulic efficiency and safety. *Tree Physiology* **40**: 215–229.

Quesada CA, Lloyd J, Schwarz M, Patiño S, Baker TR, Czimczik C, Fyllas NM, Martinelli L, Nardoto GB, Schmerler J, *et al.* 2010. Variations in chemical and physical properties of Amazon forest soils in relation to their genesis. *Biogeosciences* **7**.

Restrepo-Coupe N, da Rocha HR, Hutyra LR, da Araujo AC, Borma LS, Christoffersen B, Cabral OMR, de Camargo PB, Cardoso FL, da Costa ACL, *et al.* 2013. What drives the seasonality of photosynthesis across the Amazon basin? A cross-site analysis of eddy flux tower measurements from the Brasil flux network. *Agricultural and Forest Meteorology* **182–183**: 128–144.

Rogers A, Medlyn BE, Dukes JS, Bonan G, von Caemmerer S, Dietze MC, Kattge J, Leakey ADB, Mercado LM, Niinemets Ü, *et al.* 2017. A roadmap for improving the representation of photosynthesis in Earth system models. *New Phytologist* **213**: 22–42.

Ryan MG, Yoder BJ. **1997**. Hydraulic Limits to Tree Height and Tree Growth. *BioScience* **47**.

Sandoval D, Prentice IC. **2020**. Simple process-led algorithms for simulating habitats (SPLASH v.2.0): robust calculations of water and energy fluxes in complex terrain. *EGU General Assembly 2020* .

Santiago LS, Goldstein G, Meinzer FC, Fisher JB, Machado K, Woodruff D, Jones T. **2004**. Leaf photosynthetic traits scale with hydraulic conductivity and wood density in Panamanian forest canopy trees. *Oecologia* **140**: 543–550.

Schuldt B, Leuschner C, Brock N, Horna V. **2013**. Changes in wood density, wood anatomy and hydraulic properties of the xylem along the root-to-shoot flow path in tropical rainforest trees. *Tree physiology* **33**: 161–174.

Smith NG, Keenan TF, Prentice IC, Wang H, Wright IJ, Niinemets U, Crous KY, Domingues TF, Guerrieri R, Ishida FY, *et al.* 2019. Global photosynthetic capacity is optimized to the environment.

Sperry JS, Hacke UG, Oren R, Comstock JP. **2002**. Water deficits and hydraulic limits to leaf water supply. *Plant, Cell & Environment* **25**: 251–263.

Stangl ZR, Tarvainen L, Wallin G, Ubierna N, Räntfors M, Marshall JD. **2019**. Diurnal variation in mesophyll conductance and its influence on modelled water-use efficiency in a mature boreal Pinus sylvestris stand. *Photosynthesis Research* **141**: 53–63.

Stocker BD, Wang H, Smith NG, Harrison SP, Keenan TF, Sandoval D, Davis T, Prentice IC. **2020**. P-model v1.0: An optimality-based light use efficiency model for simulating ecosystem gross primary production. *Geoscientific Model Development* **13**: 1545–1581.

Togashi HF, Prentice IC, Evans BJ, Forrester DI, Drake P, Feikema P, Brooksbank K, Eamus D, Taylor D. **2015**. Morphological and moisture availability controls of the leaf area-to-sapwood area ratio: analysis of measurements on A ustralian trees. *Ecology and Evolution* **5**: 1263–1270.

Walker AP, Beckerman AP, Gu L, Kattge J, Cernusak LA, Domingues TF, Scales JC, Wohlfahrt G, Wullschleger SD, Woodward FI. **2014**. The relationship of leaf photosynthetic traits – Vcmax and Jmax – to leaf nitrogen, leaf phosphorus, and specific leaf area: a meta-analysis and modeling study. *Ecology and Evolution* **4**: 3218–3235.

Wang H, Prentice IC, Davis TW, Keenan TF, Wright IJ, Peng C. **2017a**. Photosynthetic responses to altitude: an explanation based on optimality principles. *New Phytologist* **213**: 976–982.

Wang H, Prentice IC, Keenan TF, Davis TW, Wright IJ, Cornwell WK, Evans BJ, Peng C. **2017b**. Towards a universal model for carbon dioxide uptake by plants. *Nature Plants 2017 3:9* **3**: 734–741.

Warton DI, Duursma RA, Falster DS, Taskinen S. **2012**. smatr 3-an R package for estimation and inference about allometric lines. *Methods in ecology and evolution* **3**: 257–259.

Wright IJ, Reich PB, Cornelissen JHC, Falster DS, Groom PK, Hikosaka K, Lee W, Lusk CH, Niinemets Ü, Oleksyn J. **2005**. Modulation of leaf economic traits and trait relationships by climate. *Global Ecology and Biogeography* **14**: 411–421.

Wright IJ, Reich PB, Westoby M. **2001**. Strategy shifts in leaf physiology, structure and nutrient content between species of high- and low-rainfall and high- and low-nutrient habitats. *Functional Ecology* **15**: 423–434.

Wright IJ, Reich PB, Westoby M. **2003**. Least-cost input mixtures of water and nitrogen for photosynthesis. *The American naturalist* **161**: 98–111.

Wright IJ, Reich PB, Westoby M, Ackerly DD, Baruch Z, Bongers F, Cavender-Bares J, Chapin T, Cornellssen JHC, Diemer M, *et al.* 2004. The worldwide leaf economics spectrum. *Nature 2004 428:6985* **428**: 821–827.

Wu J, Serbin SP, Ely KS, Wolfe BT, Dickman LT, Grossiord C, Michaletz ST, Collins AD, Detto M, McDowell NG, *et al.* 2020. The response of stomatal conductance to seasonal drought in tropical forests. *Global Change Biology* **26**: 823–839.

Xu H, Wang H, Prentice IC, Harrison SP, Wright IJ. **2021**. Coordination of plant hydraulic and photosynthetic traits: confronting optimality theory with field measurements. *New Phytologist* **232**: 1286–1296.

Yamazaki D, Ikeshima D, Sosa J, Bates PD, Allen GH, Pavelsky TM. **2019**. MERIT Hydro: A high-resolution global hydrography map based on latest topography dataset. *Water Resources Research* **55**: 5053–5073.

Yang J, He Y, Aubrey DP, Zhuang Q, Teskey RO. **2016**. Global patterns and predictors of stem CO2 efflux in forest ecosystems. *Global Change Biology* **22**: 1433–1444.

Yang Y, Wang H, Harrison SP, Prentice IC, Wright IJ, Peng C, Lin G. **2019**. Quantifying leaf-trait covariation and its controls across climates and biomes. *New Phytologist* **221**: 155–168.

Zanne AE, Lopez-Gonzalez G, Coomes DA, Ilic J, Jansen S, Lewis SL, Miller RB, Swenson NG, Wiemann MC, Chave J. **2009**. Data from: Towards a worldwide wood economics spectrum.